

Ballistic transport and interband interference in two-dimensional quantum contacts

M. V. Moskalets

93a/48, pr. Il'icha, 310020 Kharkov, Ukraine

(Submitted September 10, 1996; revised September 26, 1996)

Fiz. Nizk. Temp. **23**, 319–326 (March 1997)

A new effect, viz., the oscillatory dependence of the collector current on the diameter of the diagram confining the electron flow from the emitter to the collector, is considered. Such a dependence is due to a change in the position of conducting subbands of the diaphragms upon a change in its diameter. It is also shown that the collector current contains a noticeable interference component (associated with the Aharonov–Bohm effect and corresponding to the mixing of conduction channels of the quantum diaphragm) in the case of a strong mismatching of electron states outside and inside the diaphragm. © 1997 American Institute of Physics. [S1063-777X(97)01003-7]

INTRODUCTION

Ballistic electron transport in mesoscopic systems¹ has become an object of interest in connection with the possibility of experimental creation of controllable structures whose size is comparable with the electron wavelength λ_F , on the one hand, and due to the fact that the quantum-mechanical (wave) nature of charge carriers is manifested in such structures on the macroscopic level, on the other.

This is manifested most clearly in the conductivity of two-dimensional ballistic point contacts in the form of a narrow bridge (whose width d is comparable with λ_F) connecting two regions in a two-dimensional electron gas (see Fig. 1). It was shown experimentally in Refs. 2 and 3 that the conductance G of such a junction is quantized in the units of $G_0 = 2e^2/h$. The reason behind this is a restriction in the transverse (relative to the contact axis) motion of electrons in the microscopic constriction region, and consequently the quantization of the transverse momentum of particles.^{2–11} Each quantization level $\varepsilon_n = (\pi n \hbar / d)^2 / 2m$ ($n = 1, 2, \dots$) corresponds to the one-dimensional subband $\varepsilon_n(p_x) = p_x^2 / 2m + \varepsilon_n$ (the x axis is directed along the contact axis) with the conductance $G_n = G_0$. The number N of conducting subbands is determined by the magnitude of the Fermi energy ε_F of electrons in the banks ($x \rightarrow \pm \infty$; the junction coordinate $x = 0$) and by the contact width d which limits the separation between transverse quantization levels. The subband is conducting under the condition $\varepsilon_n < \varepsilon_F + e\varphi(d)$ [$\varphi(d)$ is the potential emerging between the junction and the banks].¹² According to the multichannel generalization of the Landauer formula,¹³ the conductance of the junction is $G = NG_0$. As the diameter d of the junction is varied, the separation between energy levels, and hence the number of conducting subband changes. Consequently, the $G(d)$ dependence has the shape of a ladder with steps of the same height G_0 .

Quantum contacts are usually described by using one of the two models: the model of a junction with a smooth geometry (adiabatic contact)^{10,11} or the model of a junction with an abrupt geometry.^{4–9} The calculations based on either of these models lead to a step dependence $G(d)$, but the

passage of an electron through the contact region differs significantly in these models. For example, in an adiabatic contact a reflectionless matching of electron states in the left and right banks is observed.¹⁰ In this case, each electron state can be unambiguously attributed to a certain conducting subband of the junction. Interband transitions associated with nonadiabaticity of the contact shape at long distances¹⁴ or with the presence of scattering centers in the junction¹⁵ only lead to small corrections for the conductance of the microscopic structure. A different situation takes place for contacts with an abrupt geometry. Mismatching of the electron states in the banks leads to a strong scattering of the electron wave in the regions of conjugation of the junction with the banks. The “backward” scattering leads to the multiple passage of the contact region by the electron wave, which is manifested in the form of the resonant structure in the $G(d)$ dependence.^{4–9} The “forward” scattering leads to the existence of several channels of transition from a certain state \mathbf{k} of the left bank to a certain state \mathbf{k}' of the right bank (via different states in the junction; see Fig. 1b) and (see below) is responsible for the interference term appearing in the expression for the transition probability $|t_{\mathbf{k},\mathbf{k}'}|^2$ ($t_{\mathbf{k},\mathbf{k}'}$ is the element of the transition matrix of the contact). Both these processes lead to a strong interband mixing. It should be noted that no resonant structure on the $G(d)$ dependence was observed in the experiments.^{2,3} This is probably due to the fact that the contacts used in these experiments have a smooth shape in view of the electrostatic nature of the potential barrier that forms the microscopic constriction. According to Castano and Kirczenow,¹⁶ the $G(d)$ dependence for nonadiabatic contacts with a smooth shape does not contain a resonant structure either. These authors emphasized a significant role of interband mixing in such contacts.

Among other things, the universal nature of quantization of conductance and its relative insensitivity to details of electron scattering in the contact is due to the fact that conductance G is determined by all electron states of the left and right banks. The expression for G has the form¹

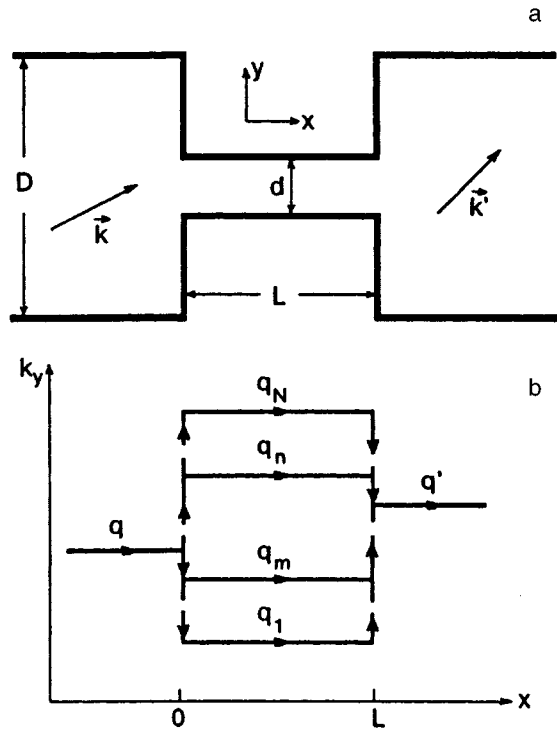


FIG. 1. (a) Model of a quantum contact of length L and width d , which connects $2D$ regions of width D ; \mathbf{k} and \mathbf{k}' are the electron wave vectors before and after the passage through the contact, respectively. (b) Phase trajectories of an electron moving through a contact; $q, q_i (1 < i \leq N)$, and q' are the projections of the electron wave vector on the x axis in front of the contact, in the contact, and behind the contact, respectively.

$$G = \frac{2e^2}{h} \text{Tr}(tt^+)_{\varepsilon_F} = \frac{2e^2}{h} \sum_{\mathbf{k}} \sum_{\mathbf{k}'} |t_{\mathbf{k}\mathbf{k}'}(\varepsilon_F)|^2. \quad (1)$$

The coefficients of transition matrix $t_{\mathbf{k}\mathbf{k}'}$ themselves contain more detailed information on electron scattering.

In the present paper, we will show that the value of $|t_{\mathbf{k}\mathbf{k}'}|^2$ can be determined by a method similar to the method of transverse electron focusing¹⁷ realized in a two-dimensional electron gas.¹⁸ It was shown theoretically in Ref. 19 that an analysis of the dependence of the collector current I_c on the magnetic field H makes it possible to reconstruct the angular distribution of electrons leaving the emitter. If we place a diaphragm between the emitter and the

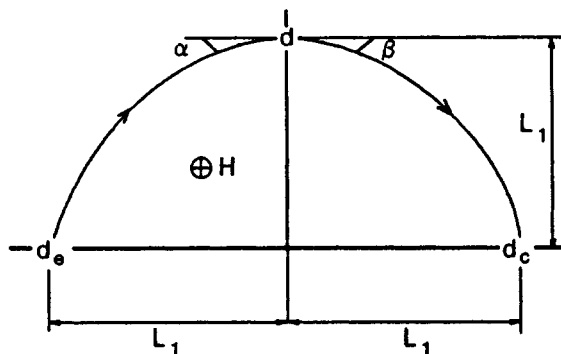


FIG. 2. Schematic diagram of mutual arrangement of the contacts.

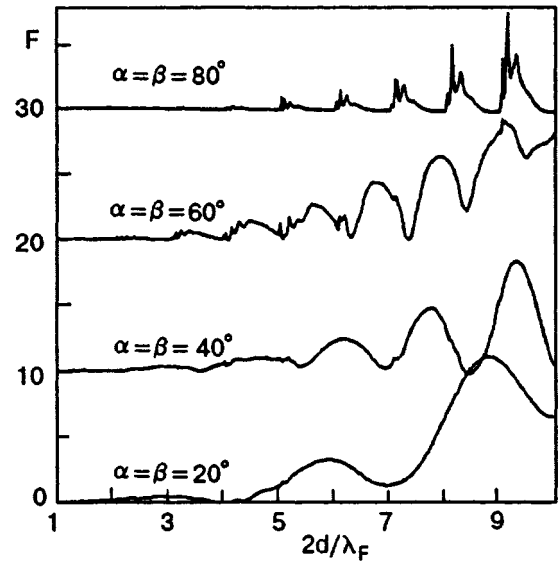


FIG. 3. Dependence of the collector current ($I_c \sim F$) on the diaphragm diameter for various angles of incidence of an electron. The value of $L/\lambda_F = 5$. For better visualization, the curves are displaced along the vertical by 0, 10, 20, and 30 rel. units and are compressed along the vertical by a factor of 6.6, 7, 3, and 0.3, respectively.

collector (Fig. 2), the collector current for a fixed value of H is proportional to the transition probability $|t_{\mathbf{k}\mathbf{k}'}|^2$ (\mathbf{k} corresponds to an electron moving from the emitter to the diaphragm, and \mathbf{k}' to an electron moving from the diaphragm to the collector). The collector current $I_c(d)$ in such a situation oscillates depending on the diaphragm diameter d . The peaks on the $I_c(d)$ dependence (Fig. 3) correspond to quantization levels of transverse motion of electrons in the region of microconstriction. Moreover, it is predicted that contacts with a sharp geometry are characterized by a significant interference contribution to I_c , which is associated with the Aharonov-Bohm electrostatic effect.²⁰

1. TRANSITION MATRIX FOR A CONTACT WITH SHARP GEOMETRY

We consider a model of a two-dimensional ballistic contact in the form of a rectangular channel of width d and length L , connecting two broad regions $D \gg d$ (Fig. 1a). The electron mean free path l is assumed to be larger than the characteristic size of the contact ($l \gg L, d$). We will describe the propagation of an electron wave through the contact by the method developed in Ref. 4.

Let us consider an electron having an energy $\varepsilon_p = p^2/(2m)$ and momentum $\mathbf{p} = \hbar\mathbf{k}$ moving through the contact (Fig. 1) from left to right (we denote $k_x \equiv \kappa$ and $k_y \equiv q$). We can write the electron wave function $\Psi_{\mathbf{k}}$ in the form

$$\left\{ \begin{array}{l} \Psi_{\mathbf{k}}(x < 0) = \chi_q(y) \exp(i\kappa x) \\ \quad + \sum_{\mathbf{k}'} r_{\mathbf{k}\mathbf{k}'} \chi_{q'}(y) \exp(-i\kappa' x), \\ \Psi_{\mathbf{k}}(0 < x < L) = \sum_n \varphi_n(y) [t_{\mathbf{k}n} \exp(i\kappa_n x) \\ \quad + r_{\mathbf{k}n} \exp(-i\kappa_n x)], \\ \Psi_{\mathbf{k}}(L < x) = \sum_{\mathbf{k}'} \tau_{\mathbf{k}\mathbf{k}'} \chi_{q'}(y) \exp(i\kappa' x). \end{array} \right. \quad (2)$$

Here $\chi_q(y)$ and $\varphi_n(y)$ are the transverse wave functions in the broad band and in the channel, respectively, which are normalized to unity. The summation is extended to all the states satisfying the energy conservation law $\varepsilon_{\mathbf{p}} = \varepsilon_{\mathbf{p}'} = \varepsilon_n + \hbar^2 \kappa_n^2 / 2m$ [in this paper, we do not consider the effect of the electrostatic potential $\varphi(d)$].¹² In addition, $\kappa > 0$ and $\kappa' > 0$. In order to define the coefficients $t_{\mathbf{k}n}$, $r_{\mathbf{k}n}$, $\tau_{\mathbf{k}\mathbf{k}'}$ and $r_{\mathbf{k}\mathbf{k}'}$, we use the continuity of the wave function (2) and of its derivative for $x=0$ and $x=L$. After simple transformations, we obtain the following system of equations for the quantities $t_{\mathbf{k}n}$ and $r_{\mathbf{k}n}$:

$$\left\{ \begin{array}{l} \sum_{\mathbf{k}'} \sum_m \kappa' a_{q'n} a_{q'm} [t_{\mathbf{k}m} \exp(i\kappa_m L) \\ \quad + r_{\mathbf{k}m} \exp(-i\kappa_m L)] = \kappa_n [t_{\mathbf{k}n} \exp(i\kappa_n L) \\ \quad - r_{\mathbf{k}n} \exp(-i\kappa_n L)], \\ \sum_{\mathbf{k}'} \sum_m \kappa' a_{q'n} a_{q'm} (t_{\mathbf{k}m} + r_{\mathbf{k}m}) \\ \quad = 2\kappa a_{qn} - \kappa_n (t_{\mathbf{k}n} - r_{\mathbf{k}n}). \end{array} \right. \quad (3)$$

Here $a_{qn} = \int_0^d dy \chi_q(y) \varphi_n(y)$ is the overlapping coefficient for transverse wave functions. The solution of this system of equations determines the coefficients $\tau_{\mathbf{k}\mathbf{k}'}$:

$$\tau_{\mathbf{k}\mathbf{k}'} = e^{-i\kappa' L} \sum_n a_{q'n} (t_{\mathbf{k}n} e^{i\kappa_n L} + r_{\mathbf{k}n} e^{-i\kappa_n L}). \quad (4)$$

Calculating the quantum-mechanical current I through a contact with a voltage $eV \ll \varepsilon_F$ applied across the banks in the standard way, at zero temperature, we obtain

$$I = \frac{2e^2}{h} V \sum_{k=k_F} \sum_{k'=k_F} \theta(\kappa) \theta(\kappa') \frac{\kappa'}{\kappa} |\tau_{\mathbf{k}\mathbf{k}'}|^2. \quad (5)$$

Here $\theta(x)$ is the unit step (Heaviside) function. Each term in expression (5) is the current passing through the contact upon a transition of an electron from the state \mathbf{k} in front of the contact to the state \mathbf{k}' behind it. Comparing the expression for the conductance $G = I/V$ obtained from (5) with expression (1), we can determine the relation between the elements of the transition matrix $t_{\mathbf{k}\mathbf{k}'}$ and the coefficients $\tau_{\mathbf{k}\mathbf{k}'}$, defining the amplitude of the wave function after the passage through the contact:

$$t_{\mathbf{k}\mathbf{k}'} = \sqrt{\kappa'/\kappa} \tau_{\mathbf{k}\mathbf{k}'}. \quad (6)$$

The quantity $|t_{\mathbf{k}\mathbf{k}'}|^2$ determines the intensity of electron flux in the state \mathbf{k}' after the passage through the contact for a unit intensity of the flux of electron in the state \mathbf{k} incident at the contact.

The solution of the system of equations (3) can be obtained only by numerical methods and requires a considerable computer time. However, Szafer and Stone⁴ used similar calculations to substantiate a method of approximate determination of coefficients $t_{\mathbf{k}n}$ and $r_{\mathbf{k}n}$ (the mean-field approximation), lying in the replacement of the exact expression for the coefficients a_{qn} by the approximate expression

$$a_{qn}^2 = \frac{d}{D} [\theta(q - q_{n-1}) - \theta(q - q_{n+1})]. \quad (7)$$

In this case, the coefficients a_{qn} must satisfy the completeness condition $\sum_q a_{qn} a_{qm} = \delta_{nm}$. It can easily be verified that using definition (7), we can assume to a sufficiently high degree of accuracy that

$$\sum_k \kappa a_{qn} a_{qm} = \delta_{nm} \sum_{q=q_{n-1}}^{q_{n+1}} \kappa = \delta_{nm} (K_n + iJ_n). \quad (8)$$

Substituting (8) into (3), we can determine the coefficients $t_{\mathbf{k}n}$ and $r_{\mathbf{k}n}$. Substituting the obtained expressions into (4), we can find the expression for the coefficients $\tau_{\mathbf{k}\mathbf{k}'}$ in the mean-field approximation:

$$\tau_{\mathbf{k}\mathbf{k}'} = \sum_{n=1}^N 2\kappa_n \kappa a_{qn} a_{q'n} Z_n^{-1} \exp(-i\kappa' L - \theta_n), \quad (9)$$

where

$$Z_n^2 = 4K_n^2 \kappa_n^2 + [(K_n + \kappa_n)^2 + J_n^2][(K_n - \kappa_n)^2 + J_n^2] \sin^2(\kappa_n L + \varphi_n), \quad (10)$$

$$\tan \varphi_n = 2J_n \kappa_n (K_n^2 - \kappa_n^2 + J_n^2)^{-1}, \quad (11)$$

$$(\tan \theta_n) = \frac{2J_n \kappa_n \cos(\kappa_n L) - (K_n^2 + \kappa_n^2 - J_n^2) \sin(\kappa_n L)}{2K_n [\kappa_n \cos(\kappa_n L) + J_n \sin(\kappa_n L)]}. \quad (12)$$

Expression (9) shows that the amplitude of transmitted wave ($\tau_{\mathbf{k}\mathbf{k}'}$) consists of N terms corresponding to the existence of N possible channels through a contact, namely, to an electron transition to a certain conducting subband of the contact (see Fig. 1b) (for $L/\lambda_F \gg 1$, the contribution of attenuating modes $n > N$ can be neglected). The contribution from each possible channel of the transition is proportional to the product of the overlapping coefficients $a_{qn} a_{q'n}$. It should be noted that the mean-field approximation (7) and (8) can be applied only for solving the system of equations (3). The quantity θ_n is the phase shift of the electron wave during its passage through the contact in the subband with the number n . For deep energy levels (actually for $n \leq N-1$), we have

$$\theta_n = -(1 - (n\lambda_F/2d)^2)^{1/2} k_F L. \quad (13)$$

The motion in the subband can be regarded as the motion in the region with the potential energy $\varepsilon_n = (\pi n \hbar / d)^2 / (2m)$. Thus, a multichannel analog of the Aharonov-Bohm electrostatic effect is realized in this situation.

While calculating the value of quantities quadratic in $\tau_{\mathbf{k}\mathbf{k}'}$ [such as the current (5)], we encountered interference terms associated with the splitting of the electron wave en-

tering the channel and with subsequent interference of transmitted waves emerging from the channel (see Fig. 1b). Interference is possible in the absence of inelastic processes which destroy the coherent electron state, which we are assuming here.

Further, substituting (9) into (6), we obtain an expression for the quantities $|t_{\mathbf{k}\mathbf{k}'}|^2$ in the form

$$|t_{\mathbf{k}\mathbf{k}'}|^2 = \sum_{n=1}^N 4\kappa_n^2 \kappa \kappa' a_{qn}^2 a_{q'n}^2 Z_n^{-2} + 2 \sum_{n=2}^N \sum_{m=1}^{n-1} 4\kappa_n \kappa_m \kappa \kappa' \times a_{qn} a_{q'n} a_{qm} a_{q'm} Z_n^{-1} Z_m^{-1} \cos(\theta_n - \theta_m). \quad (14)$$

The first term corresponds to the additive contribution of the conducting subbands to the transition probability, while the second is the interference term. Its sign is determined by the difference in the phase lead in different subbands as well as by the phase jump at the entrance and at the exit of the channel, i.e., by the signs of the quantities a_{qn} .

In the next section, we will consider the schematic diagram of an experiment which makes it possible to determine the coefficients $|t_{\mathbf{k}\mathbf{k}'}|^2$ directly.

2. COLLECTOR CURRENT IN THE PRESENCE OF A QUANTUM DIAPHRAGM

Let us consider the ballistic propagation of electrons from the emitter to the collector separated by a diaphragm in a weak magnetic field (see Fig. 2). The diaphragm was in the form of a quantum contact with the elements of transition matrix $t_{\mathbf{k}\mathbf{k}'}$, while the collector and the emitter were classical point contacts. When the current I_e was passed through the emitter, a fraction of nonequilibrium electrons scattered by the diaphragm reaches the collector creating the collector current I_c (we assume that electrons cannot move directly from the emitter to the collector). For the mutual arrangement of the contact shown in Fig. 2, the expression for the collector current can be written in the form

$$I_c = I_e \int_{\alpha_2}^{\alpha_1} d\alpha \int_{\beta_2}^{\beta_1} d\beta \cos \alpha \cos \beta |t(\alpha, \beta)|^2. \quad (15)$$

Here $t(\alpha, \beta) = (D/\lambda_F) t_{\mathbf{k}\mathbf{k}'}$;

$$\alpha_{1,2} = \arccos\{[1 + (1 \mp d/2L_1)^2]^{1/2} L_1/2r_H\} - \arccos\{[1 + (1 \mp d/2L_1)^2]^{-1/2}\};$$

$$\beta_{1,2} = \arccos\{[1 + (1 \mp d_c/2L_1)^2]^{1/2} L_1/2r_H\} - \arccos\{[1 + (1 \mp d_c/2L_1)^2]^{-1/2}\};$$

$2L_1$ is the separation between the contacts, $r_H = cp_F/(eH)$ is the cyclotron radius, and d and d_c are the diameters of the diaphragm and the collector, respectively. We assume that the following conditions are satisfied: $l, r_H > L_1 > d_c, d_e > d \approx \lambda_F$ (d_e is the diameter of the emitter).

In experiments (see, for example, Ref. 18), the voltage V_c which must be applied to the collector for the total collector current to be equal to zero ($I_c - V_c/R_c = 0$, where R_c is the resistance of the collector) is usually measured. It should be noted that in the case of a linear response ($eV_c \ll \varepsilon_F$), the value of I_c does not depend on the voltage across the collector. For a small value of the ratio d/L_1 and d_c/L_1 , we can

factor $t(\alpha, \beta)$ outside the integral sign in (15) and using (14), we can obtain the following expression for the voltage across the collector:

$$V_c = I_e R_c \frac{\lambda_F d_c}{16L_1^2} \left[1 + \cot\left(\alpha + \frac{\pi}{4}\right) \right] \left[1 + \cot\left(\beta + \frac{\pi}{4}\right) \right] F, \quad (16)$$

where $\alpha = \beta = \arccos(L_1/\sqrt{2}r_H) - \pi/4$. Since $\kappa = k_F \cos \alpha$, $q = k_F \sin \alpha$, $\kappa' = k_F \cos \beta$, and $q' = k_F \sin \beta$, we find that the expression for $F = F_0 + F_i$ has the form

$$F_0 = \sum_{n=1}^N 2\xi \kappa_n^2 k_F^2 Z_n^{-2} \varphi(n, n). \quad (17)$$

$$F_i = \sum_{n=2}^N \sum_{m=1}^{n-1} 4\xi \kappa_n \kappa_m k_F^2 Z_n^{-1} Z_m^{-1} \varphi(n, m) \cos(\theta_n - \theta_m), \quad (18)$$

$$\varphi(n, m) = a_n(\alpha) a_m(\alpha) a_n(\beta) a_m(\beta) \cos^2 \alpha \cos^2 \beta, \quad (19)$$

where $\xi = 2d/\lambda_F$; $\kappa_n = k_F(1 - (n/\xi)^2)^{1/2}$, and

$$a_n(\alpha) = \frac{\sqrt{2n} \sin[\pi\xi(\sin \alpha - \sin \alpha_n)]}{\pi\xi^{3/2} \sin^2 \alpha - \sin^2 \alpha_n}, \quad (20)$$

where $\alpha_n = \arcsin(n\lambda_F/2d)$.

3. DEPENDENCE OF THE COLLECTOR CURRENT ON THE DIAPHRAGM DIAMETER

Figure 3 shows the dependence of the quantity F which appears in expression (16) and which defines the voltage V_c across the collector (or the collector current $I_c = V_c/R_c$) on the diaphragm diameter d . The presence of peaks on the $I_c(d)$ [accordingly, $V_c(d)$] dependence is mathematically due to the vanishing of the denominator of the overlapping coefficient $a_n(\alpha)$ (20). The physical origin of these phenomena is as follows. The quantity $a_n(\alpha)$ has a peak for $\alpha = \alpha_n$, which corresponds to the coincidence of transverse wave vectors $q_n = \pi n/d$ in the contact (in the n th subband) and $q = k_F \sin \alpha$ outside the contact. A change in the diaphragm diameter d leads to a change in the position of quantization levels in the microscopic constriction, and the condition $q = q_n$ is observed for a certain $d = d_n$. At this instant, the resonant mode of electron passage through the microconstriction is realized in the n th subband, leading to an increase in the collector current. The positions of the peaks are determined by the expression

$$d_n = \frac{\lambda_F}{2} \frac{n}{\sin \alpha}. \quad (21)$$

The fine structure of the peaks is associated with two effects: the intraband and interband interference. The interference of electron waves in a conducting subband is associated with "backward" scattering at the channel edges, which is responsible for multiple passage of the electron wave through the region of microscopic constriction. This effect is described by the quantity Z_n (10) in expressions (17) and (18) and is manifested in the form of a resonant structure on the $G(d)$ dependence for contacts with a sharp shape.⁴⁻¹¹ A peculiar feature of this effect is that the resonant structure is

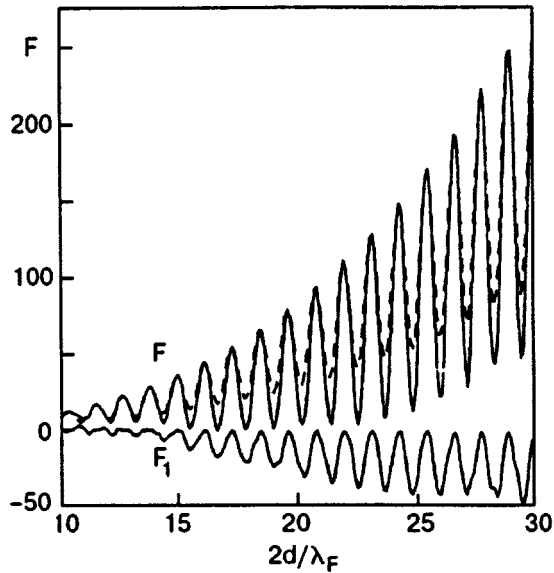


FIG. 4. Collector current ($I_c \sim F$) in the case of large diaphragm diameter for $\alpha = \beta = 60^\circ$, $L/\lambda_F = 5$. The dashed curve corresponds to the quantity F_0 (17). The curves are compressed along the vertical by a factor of 3.

determined by the contribution from the upper conducting subband alone since the $Z_n(d)$ dependence is smooth for $n < N$. It follows from (21) that the number n of a resonant level is connected with the number $N = [2d/\lambda_F]$ in the contact through the relation $N = [n/\sin \alpha]$ (the brackets indicate the integral part of a number). It can be seen from Fig. 3 that $n = N$ for $\alpha \approx \pi/2$, i.e., the main contribution to the collector current comes from the upper conducting subband; for this reason, the peak is strongly jagged (for $L/d \gg 1$). As the angle α decreases, the peak is smoothed since the main role is played by deeper energy levels.

The contribution of interband interference to the collector current is defined by Eq. (18). This contribution is significant when a large number of subbands in the microconstriction are conducting. However, for $\alpha \approx \pi/2$, this contribution is insignificant since the separation between quantization levels in the vicinity of the upper conducting subband (which determines the main contribution to the current in the given case) is large, and the product $a_n(\alpha)a_m(\alpha)$ ($n \neq m$) is small. Figure 4 shows the dependence of the quantities F , F_0 , and F_i on the contact diameter in the region $d \gg \lambda_F/2$. It can be seen that the contribution from interband interference processes considerably affects the shape of the curve.

In the region $d \approx \lambda_F/2$, the peculiarities associated with the two effects are superimposed (Fig. 5a). If, however, we take into account the effect of temperature T , i.e.,

$$|t_{\mathbf{k}\mathbf{k}'}(T)|^2 = - \int d\varepsilon f'(\varepsilon, T) |t_{\mathbf{k}\mathbf{k}'}(\varepsilon)|^2 \quad (22)$$

[$f(\varepsilon, T)$ is the Fermi distribution function], the peculiarities associated with the intraband interferences are smoothed even for $T = 0.01\varepsilon_F$ (Fig. 5b).

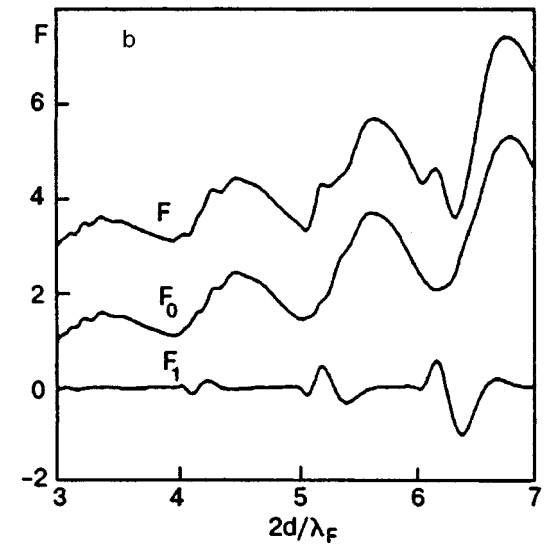
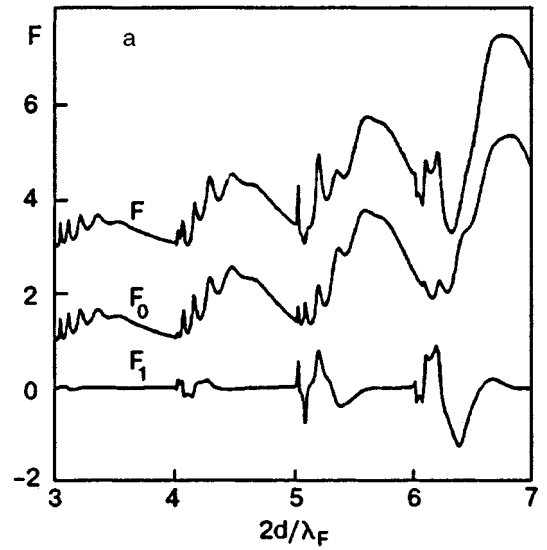


FIG. 5. Dependence of the collector current ($I_c \sim F$) on the diaphragm diameter for $\alpha = \beta = 60^\circ$, $L/\lambda_F = 5$ at various temperatures: $T = 0$ (a) and $T = 0.01\varepsilon_F$ (b). The curves are displaced along the vertical by 0.1 and 3 rel. units, respectively, and compressed by a factor of 3.

CONCLUSIONS

We have considered the conductivity of a ballistic microscopic structure consisting of an emitter, a collector, and a quantum diaphragm. It is shown that the current in such a system oscillates with a change in the diaphragm diameter. This is due to the resonant passage of an electron through the microconstriction in the case where the transverse momentum of an impinging electron coincides with the momentum corresponding to one of the quantum energy levels in the microconstriction.

It should be noted that the contribution from electrons reflected from the confining surfaces is not taken into account in expression (15). This contribution is small in weak magnetic fields (is absent for $H = 0$) and is manifested in the form of a smooth background on the $V_c(d)$ dependence.

The scattering of an electron wave at the entrance and the exit of the microconstriction ("forward" scattering)

leads to the emergence of a coherent state corresponding to the passage of the contact over all conducting subbands (see Fig. 1b). The interference of transmitted waves affects the collector current [see (18)]. In this case, the phase shift of the wave $\theta_n \simeq -L(k_F^2 - (\pi n/d)^2)^{1/2}$ is different for different subbands and depends on the contact diameter d . This effect is a multichannel analog of the Aharonov–Bohm electrostatic effect.

We have investigated a diaphragm with rectangular edges. Collector current oscillations should be present, however, in the case of an adiabatic contact (playing the role of a diaphragm) also. The only difference lies in the absence of interference contributions, which is manifested in a smoother shape of the peaks.

¹Y. Imry, in *Physics of Mesoscopic Systems: Directions in Condensed Matter Physics* (ed. by G. Grinstein and G. Mazenko), World Scientific, Singapore (1986).

²B. J. van Wees, H. van Houten, C. W. J. Beenakker *et al.*, Phys. Rev. Lett. **60**, 848 (1988).

³D. A. Wharam, T. J. Thornton, R. Newbury *et al.*, J. Phys. **C21**, L209 (1988).

⁴A. Szafer and A. D. Stone, Phys. Rev. Lett. **62**, 300 (1989).

⁵G. Kirczenow, Phys. Rev. **B39**, 10452 (1989).

⁶I. B. Levinson, Pis'ma Zh. Éksp. Teor. Fiz. **48**, 273 (1988) [JETP Lett. **48**, 301 (1988)].

⁷L. Escapa and N. Garsia, J. Phys. Condens. Matter. **1**, 2125 (1989).

⁸D. van der Marel and E. G. Haanappel, Phys. Rev. **B39**, 7811 (1989).

⁹A. M. Zagoskin and I. O. Kulik, Fiz. Nizk. Temp. **16**, 911 (1990) [Sov. J. Low Temp. Phys. **16**, 533 (1990)].

¹⁰L. I. Glazman, G. B. Lesovik, D. E. Khmel'nitskii, and R. I. Shekhter, Pis'ma Zh. Éksp. Teor. Fiz. **48**, 218 (1988) [JETP Lett. **48**, 238 (1988)].

¹¹A. Kawabata, J. Phys. Soc. Jpn. **58**, 372 (1989).

¹²M. V. Moskalets, Pis'ma Zh. Éksp. Teor. Fiz. **62**, 702 (1995) [JETP Lett. **62**, 719 (1995)].

¹³M. Büttiker, Y. Imry, R. Landauer, and S. Pinhas, Phys. Rev. **B31**, 6207 (1985).

¹⁴A. Yacoby and Y. Imry, Phys. Rev. **B41**, 5341 (1990).

¹⁵A. M. Zagoskin and R. I. Shekhter, Phys. Rev. **B50**, 4909 (1994).

¹⁶E. Castano and G. Kirczenow, Phys. Rev. **B45**, 1514 (1992).

¹⁷V. S. Tsoi, Pis'ma Zh. Éksp. Teor. Fiz. **19**, 114 (1974) [JETP Lett. **19**, 70 (1974)].

¹⁸H. van Houten, C. W. J. Beenakker, J. G. Williamson *et al.*, Phys. Rev. **B39**, 8556 (1989).

¹⁹M. V. Moskalets, Pis'ma Zh. Éksp. Teor. Fiz. **63**, 604 (1996) [JETP Lett. **63**, 639 (1996)].

²⁰Y. Aharonov and D. Bohm, Phys. Rev. **115**, 484 (1959).

Translated by R. S. Wadhwa